Towards Finger Motion Capture System Using FBG Sensors

Minsu Jang, Jun Sik Kim, Kyumin Kang, Jinseok Kim, and Sungwook Yang, *Member, IEEE*

***Abstract*—This paper introduces a novel finger motion capture system using FBG (fiber Bragg grating) optical sensors. We develop two types of sensors to seamlessly reconstruct finger motion from strains induced in the FBGs. First, the shape sensor incorporates three optical fibers with multiple FBGs to reconstruct the position and orientation of a finger joint in 3D. In addition, the angle sensor is designed to measure the high curvature of bending on the finger joints. By deploying the two types of sensors on the fingers, we can reconstruct various finger motion in real time without drift over time. The accuracies of the fabricated FBG sensors are evaluated, resulting in an average error of 1.49 mm for the shape sensor at the distal tip (1.9% for the full length of the sensor) and 0.21° error for the angle sensor. We finally demonstrate finger motion tracking with the FBG sensors in real time, while measuring the multi-DOF motion at the carpometacarpal joint of the thumb and also the high curvatures of bending motion at the metacarpophalangeal and interphalangeal joints of the thumb and the index finger.**

I. Introduction

The analysis of hand movement has increasingly gained attention in a variety of biomedical application, such as biomechanical study [1], patient monitoring [2], rehabilitation [3], and neurophysiology [4]. In particular, real-time finger motion tracking is important in quantitative evaluation of pathologic effects on hand functions, planning of surgical intervention, effective rehabilitation therapy, and physiological understanding [5]. However, tracking hand motion is still challenging compared to other gross body motions, due to fine motor control and complicated movement: the total 21 degree-of-freedom (DOF) except the wrist [6].

Wearable systems have been introduced for tracking finger motion with various modalities of sensors: magnetic [7], inertial [8], or optical fiber sensors [9]–[12]. Such data gloves facilitate recognition of hand motion, while addressing complications observed in camera-based systems: the limited spatial extent and line-of-sight obstruction [13]. For example, magnetic sensors provide high resolution in estimation of hand gestures. However, its sensor signal is prone to interference with any ferromagnetic objects close to the system. The great advantages of inertial sensing systems, often called IMUs, are the usability and portability of the systems. However, the inertial sensing systems may suffer from drift in measurement due to accumulation of error in processing. Moreover, installing IMUs on each finger segment would be bulky, which could hinder natural hand pose and grasp.

As an alternative, motion tracking systems based on optical fiber sensors [9]–[12] have a great deal of advantages, such as ultrathin, flexible and lightweight natures of the systems, structural robustness, immunity to electromagnetic interference. Nevertheless, these systems are still not suitable for seamlessly tracking finger motion with multiple degrees-of-freedom. For instance, a system using hetero-cored optical fibers detects the optical loss of the light, leaking through the hetero-cored regions upon finger flexion [9]. However, this system may result in fragility issues because of the weak splicing region between two different fiber cores. Although multi-cored optical fiber sensors can measure bending motion with high curvatures, the system may also cause problems such as out of focus of light at the different location of each core and difficulties in coupling multi-cored fibers [10]. On the other hand, the systems based on fiber Bragg gratings (FBGs) could address those issues, as the systems keep the same diameter, and multiple signals at different center wavelengths of the FBGs can be simultaneously detected. For instance, Da Silva et al. introduced a sensorized glove using an FBG optical fiber in response to mechanical strain change [11]. They demonstrated close and opening hand gestures by measuring strains experienced in a single FBG fiber placed over the glove. However, the system was designed primarily for measuring the flexion and extension of finger movements only. Moon *et al*. presented a 3D shape sensor incorporating a circular array of three optical fibers with multiple FBGs [12]. They investigated the measurable curvatures of the sensor; the diameter of the sensor significantly affects the detection limit of curvatures. Accordingly, these types of FBG sensors would

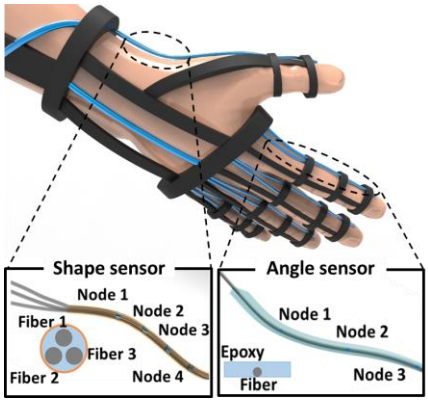

Figure 1. Illustration of the finger motion capture system using FBG sensors and exemplary installation of the sensors on the thumb and the index finger.

* This work was supported by the Global Frontier R&D Program on <Human-centered Interaction for Coexistence> funded by the National Research Foundation of Korea grant funded by the Korean Government (MEST) (NRF-2015M3A6A3076511).

M. Jang is with the Center for Bionics, Korea Institute of Science and Technology, Seoul 02792, Korea and also with School of Chemical Engineering, Sungkyunkwan University, Suwon, 16419, Korea.

J. S. Kim, K. Kang, and J. Kim are with the Center for Bionics, Korea Institute of Science and Technology, Seoul 02792, Korea (corresponding author to provide phone: 82-2-958-6745; fax: 82-2-958-6446; e-mail: jinseok@kist.re.kr).

S. Yang is with the Center for BioMicrosystems, Korea Institute of Science and Technology, Seoul 02792, Korea (corresponding author to provide phone: 82-2-958-5747; fax: 82-2-958-6910; e-mail: swyang@kist.re.kr).

not be applicable to finger motion tracking that involves relatively high curvatures on the finger joints.

In this paper, we introduce a novel finger motion capture system using FBG sensors as shown Fig. 1. The proposed system incorporates two different types of the FBG sensors, i.e., the shape and angle sensors, to measure various finger motions. Specifically, the shape sensor is used to measure two degrees-of-freedom (DOF) motion on the carpometacarpal joint. In addition, the angle sensor is used to measure 1-DOF bending motion (flexion/extension) with high curvatures at the interphalangeal and metacarpophalangeal joints, indicated in Fig. 1. Finally, we demonstrate real-time finger motion tracking, while installing these sensors on the thumb and the index finger as a pilot study.

II. Materials and Methods

A. Fiber Bragg Grating(FBG) Principle

A fiber Bragg grating (FBG) is a type of distributed Bragg reflector segmented in an optical fiber that reflects particular wavelengths of light, while transmitting all others. Given a broadband spectrum light, constructive interference occurs only at a specific wavelength of light, called the Bragg wavelength as in (1);

$$\lambda_b = 2n\Lambda\,, \tag{1}$$

where n is the refractive index of an optical fiber core and Λ is the periodic grating pitch [14]. Hence, multiple FBGs can be inscribed in a single fiber with various Bragg wavelengths, since difference FBGs reflect unique wavelengths of light.

The change of a Bragg wavelength can be approximated by (2) according to changes in strain and temperature.

$$\frac{\Delta\lambda_b}{\lambda_b} = (1-\rho_e)\varepsilon + (\alpha_\Lambda + \alpha_n)\Delta T \tag{2}$$

The first term in (2) describes the effect of strain on the wavelength shift, where ρ_e is the strain-optic coefficient and ε is the strain experienced by the grating. The latter term is given by the thermal effect on the wavelength shift. The thermal expansion coefficient and the thermo-optic coefficient for the core of the optical fiber are denoted by α_Λ and α_n, respectively. The wavelength shift by change in temperature is due primarily to the thermo-optic coefficient, since the thermal expansion coefficient of glass is practically negligible. Therefore, the wavelength change with respect to the center wavelength, $\Delta\lambda_b / \lambda_b$, is assumed to be proportional only to the stain of the fiber at room temperature.

B. FBG Sensor Design and Fabrication

We introduce two different types of the FBG sensors, i.e., the shape and angle sensors, to measure various finger motions. First, the shape sensor incorporates a circular array of multiple optical fibers to measure 2D strains induced on the cross section of each FBG node. Each fiber has five FBG nodes of an 8 mm-length with a spacing of 20 mm (FBGS Technologies GmbH, Germany). Since each FBG has different Bragg wavelength, the sensor can simultaneously detect multiple strains at different nodes on a single fiber. For fabrication of the shape sensor, we first insert the fibers into a

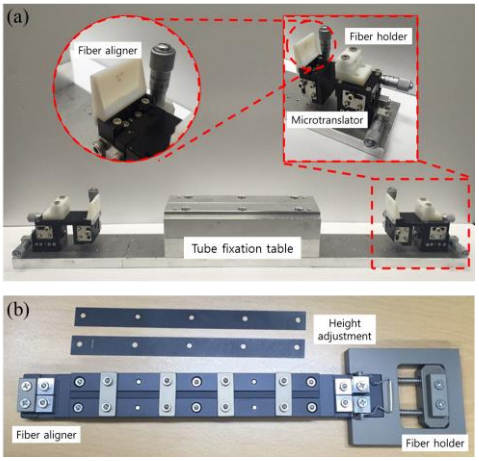

Figure 2. Fabrication of FBG sensors and alignment jig fixtures (a) and (b).

polyimide tubing with an inner diameter of 300 μm and 120 mm long. To keep the same offset distance of each fiber from the neutral axis of bending, we firmly fix the tubing and hold the fibers at the both ends of an alignment jig fixture as shown in Fig. 2. An epoxy adhesive (EPO-TEK® 301, Epoxy Technology Inc., USA) is then injected into the tubing to immobilize the fibers.

The angle sensor is designed to measure high curvatures of bending. We use a single fiber instead of multiple fibers, in order to minimize a distance between the optical fiber and the neutral axis of bending; minimizing the distance in the shape sensor is limited fundamentally by the diameter of the fibers and the arrangement of the circular array. Accordingly, the angle sensor measures 1D strain induced on the cross section of the fiber, allowing for reconstruction of the 1-DOF bending motion at each FBG node. For fabrication of the angle sensor, we locate a fiber that has three FBG nodes with a spacing of 20 mm, in the middle of the jig fixture. Then, the fixture is then fully assembled with a feeler gauge to adjust a specific thickness of the sensor; the corresponding thickness is thus set to be 250 μm, resulting in a distance offset of 67 μm from the neutral axis of the sensor. The angle sensor is 150 mm wide and 100 mm long. The epoxy is finally poured in the gap between the walls of the jig fixtures. It is then cured for 1 hour at 65°C under a certain pressure

C. FBG Sensor 3D Shape Reconstruction

The strain ε_x induced in each FBG node is described by $-\kappa d$, where κ is the curvature of the fiber and d is a distance offset from the neutral axis of bending at the cross section of the sensor. For the circular array of multiple fiber sensor, we define the strain induced in the *k*th fiber at the *i*th node, ε_i^k, as the projection of the entire strain onto each fiber as in (3).

$$\varepsilon_i^k = \kappa_i^{FBGs} d_i^k \cos(\theta_i^{FBGs} - \theta_i^k) \tag{3}$$

κ_i^{FBGs} is the curvature of the sensor and θ_i^{FBGs} is the direction of bending at the *i*th node. The arrangement of the *k*th fiber at the *i*th node is represented by d_i^k and θ_i^k, where d_i^k is the distance of the *k*th FBG node from the neutral axis and θ_i^k is

the angle of rotation from the *y*-axis of the sensor (bending direction).

For the total K number of FBG fibers in a sensor, we can formulate ε_i^k / d_i^k in terms of $\kappa_i^{FBGs}\cos\theta_i^{FBGs}$ and $\kappa_i^{FBGs}\sin\theta_i^{FBGs}$ as in (4).

$$\begin{bmatrix} \frac{\varepsilon_i^1}{d_i^1} \\ \vdots \\ \frac{\varepsilon_i^K}{d_i^K} \end{bmatrix} = \begin{bmatrix} \cos\theta_i^1 & \sin\theta_i^1 \\ \vdots & \vdots \\ \cos\theta_i^K & \sin\theta_i^K \end{bmatrix} \begin{bmatrix} \kappa_i^{FBGs}\cos\theta_i^{FBGs} \\ \kappa_i^{FBGs}\sin\theta_i^{FBGs} \end{bmatrix} \tag{4}$$

From (4), we can find both the magnitude κ_i^{FBGs} and direction θ_i^{FBGs} of the curvature on the cross section of the sensor. For example, the angle sensor retrieves the magnitude of the curvature, where it is assumed that the bending of the fiber always occur along *y*-axis of the sensor. With the assumption of $\theta_i^{FBGs} \simeq \theta_i$ in (3), it yields a simplified relationship, $\kappa_i^{FBGs} = \varepsilon_i / d_i$.

Given the magnitude and direction of the curvatures, we can retrieve the shape and the angle of FBG sensors using the Frenet–Serret formulas, which describes a particle moving along a continuous curve with three orthonormal bases in $\mathbb{R}^3$. The orthonormal bases are described by the tangent, normal, and binormal unit vectors, often called **T**, **N**, and **B** (or TNB frames). The formulas are as follows:

$$\begin{aligned} \frac{d\mathbf{T}(s)}{ds} &= \kappa\mathbf{N}(s), \\ \frac{d\mathbf{N}(s)}{ds} &= -\kappa\mathbf{T}(s) + \tau\mathbf{B}(s), \\ \frac{d\mathbf{B}(s)}{ds} &= -\tau\mathbf{N}(s), \end{aligned} \tag{6}$$

where d / ds is the derivative with respect to arc length. κ is the curvature, and τ is the torsion of the curve. The torsion is defined by $\tau = d\psi / ds$, where $d\psi$ is the angle between the positive directions of the binormals of the curve. Herein, the torsion is assumed to be zero for angle sensors. We finally obtain the position vector of each interpolated segment $\mathbf{R}(s)$ by integrating the unit tangent vector, $\mathbf{T} = d\mathbf{R} / ds$, over the total length of the curve. The angle of each segment, θ_s, is also defined by two adjacent vectors: $\theta_s = \text{atan2}(\Delta R_y, \Delta R_x)$.

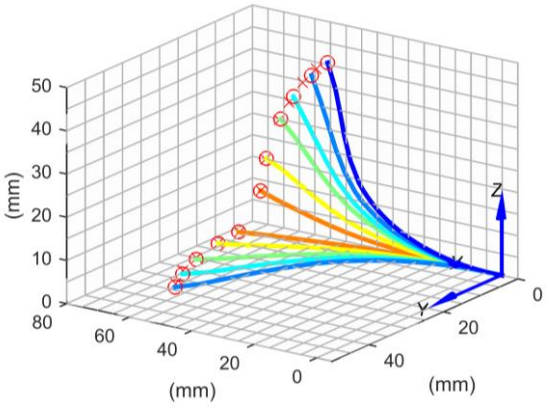

Figure 3. Reconstructed paths of the shape sensor for various target positions in the *xy* and *xz* planes. The crosses indicate target positions.

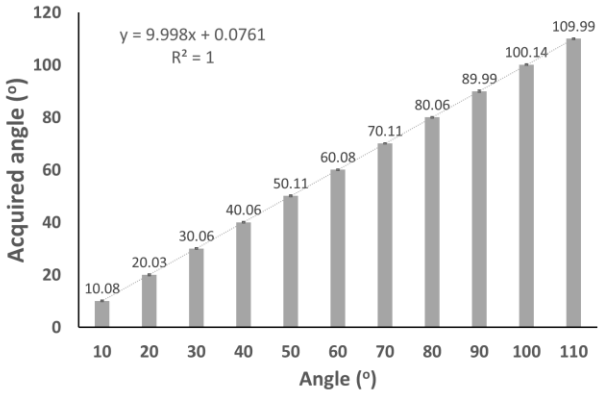

Figure 4. Evaluation of FBG angle sensors for various target angles.

D. Finger Motion Capture System

The peak wavelengths of the FBGs are detected by an optical signal interrogator (NI PXIe-4844, National Instruments). A graphical user interface (GUI) allows for real-time visualization of hand gestures and also for monitoring an individual sensor. To retrieve finger motion with the fabricated FBG sensors, we deploy the two types of the sensors on the thumb and index, using bend-typed attachments fabricated by 3D printing. These bend-typed attachments can thus accommodate different hand sizes, regardless of variation of users. For the thumb, the shape sensor is used to measure complicated movement of a carpometacarpal joints (CMC joint). In addition, we also deploy two angle sensors on a metacarpophalangeal and an interphalangeal joints in order to measure each 1-DOF angular motion. For the index finger, three angle sensors are used: the two for two interphalangeal joints between phalanges (DIP and PIP joints), and the other for the metacarpophalangeal joint (MCP joint).

III. Experiments and Results

A. FBG Sensor Evaluation

Before installation of the shape sensor and the angle sensors on the fingers, we measured the accuracies of the sensors. First, the shape sensor was placed on two orthogonal planes, *xy*- and *xz*-plane. The distal end of the sensor was located on specific positions marked on a graph paper. We then compared the measured tip position with the target position marked as crosses in Fig. 3. For the small range of motion, accurate measurement was obtained. However, for the gross motion, the larger error was observed as the overall curvature of the sensor increases. The overall error for the entire measurement was 1.49 mm, which is 1.9 % of the total length of the sensor. The distortion of wavelength spectrum appeared above a bending curvature of 0.02 mm^{-1} for the shape sensor. We also evaluated the accuracy of the angle sensor for a small radius of curvature possibly created by various hand motions: 12 mm corresponding to a bending curvature of 0.083 mm^{-1}. The angle sensor could robustly measure various angles within a range of 0.0°– 110.0, while resulting in an error of 0.21° without significant distortion of the reflection spectrum as shown in Fig 4.

Figure 5. Demonstration of the finger motion capture system in real time: tracking the index finger (a), the thumb (b), and both the fingers (c).

B. *Finger Motion Tracking*

We finally demonstrate real-time tracking of finger motion with the developed FBG sensors and system. The representative finger motions are presented in Fig. 5 with corresponding tracking results. The GUI visualizes the poses of the fingers and also provides the resulting angles of the finger joints in real time. The flexion/extension movement of the index finger is demonstrated in Fig. 5(a) and the abduction/adduction and the flexion/extension of the CMC joint are in Fig. 5(b). Fig. 5(c) presents various hand gestures while simultaneously moving the thumb and the index fingers. As a result, the proposed system could track the user's various hand gestures with the FBG sensors developed, although the application of all finger movements and quantitative analysis are not available yet.

IV. Discussion

We presented a new finger motion tracking system using FBG fiber sensors. The new system measures the strains induced on the FBG nodes and then reconstruct the entire shape of the finger segments. The shape sensor deployed on the CMC joint is thus capable of measuring the multi-DOF motion of the joint. In addition, the angle sensor is suitable for such small radii of curvatures at interphalangeal joints for various finger movement. The proposed system also shows notably better performance, compared to the markerless hand motion capture system that reported a maximum error level of 10° [13].

Further development is still required for tracking entire hand motion in real time. First of all, the data processing and visualization platforms should be modified for fast hand motion tracking. The tracking speed is currently limited by the optical sensor interrogator used and the GUI based on the Matlab™ platform. We will also apply the shape sensors on the MCP joints in addition to the angle sensors currently used. This would thus enables to measure all degrees-of-freedom at the MCP joints including abduction and adduction motions.

References

[1] P. Braido and X. Zhang, "Quantitative analysis of finger motion coordination in hand manipulative and gestic acts," *Hum. Mov. Sci.*, vol. 22, no. 6, pp. 661–678, 2004.

[2] R. Agostino, A. Currà, M. Giovannelli, N. Modugno, M. Manfredi, and A. Berardelli, "Impairment of individual finger movements in Parkinson's disease," *Mov. Disord.*, vol. 18, no. 5, pp. 560–592, 2003.

[3] H. Zhou and H. Hu, "Human motion tracking for rehabilitation-A survey," *Biomed. Signal Process. Control*, vol. 3, no. 1, pp. 1–18, 2008.

[4] U. Castiello, "The neuroscience of grasping," *Nat. Rev. Neurosci.*, vol. 6, no. 9, pp. 726–736, 2005.

[5] P. Cerveri, E. De Momi, N. Lopomo, G. Baud-Bovy, R. M. L. Barros, and G. Ferrigno, "Finger kinematic modeling and real-time hand motion estimation," *Ann. Biomed. Eng.*, vol. 35, no. 11, pp. 1989–2002, 2007.

[6] J. Lin, Y. Wu, and T. S. Huang, "Modeling the constraints of human hand motion," in *Proceedings Workshop on Human Motion*, 2000, pp. 121–126.

[7] Y. Ma, Z. H. Mao, W. Jia, C. Li, J. Yang, and M. Sun, "Magnetic hand tracking for human-computer interface," *IEEE Trans. Magn.*, vol. 47, no. 5, pp. 970–973, 2011.

[8] B. S. Lin, P. C. Hsiao, S. Y. Yang, C. S. Su, and I. J. Lee, "Data glove system embedded with inertial measurement units for hand function evaluation in stroke patients," *IEEE Trans. Neural Syst. Rehabil. Eng.*, vol. 25, no. 11, pp. 2204–2213, 2017.

[9] M. Nishiyama and K. Watanabe, "Wearable sensing glove with embedded hetero-core fiber-optic nerves for unconstrained hand motion capture," *IEEE Trans. Instrum. Meas.*, vol. 58, no. 12, pp. 3995–4000, 2009.

[10] J. P. Moore and M. D. Rogge, "Shape sensing using multi-core fiber optic cable and parametric curve solutions," *Opt. Express*, vol. 20, no. 3, p. 2967, 2012.

[11] A. F. Da Silva *et al.*, "FBG sensing glove for monitoring hand posture," *IEEE Sens. J.*, vol. 11, no. 10, pp. 2442–2448, 2011.

[12] H. Moon, J. Jeong, O. Kim, K. Kim, W. Lee, and S. Kang, "FBG-based polymer-molded shape sensor integrated with minimally invasive surgical robots," in *Proc. IEEE Conference on Robotics and Automation*, 2015, pp. 1770–1775.

[13] C. D. Metcalf *et al.*, "Markerless motion capture and measurement of hand kinematics: Validation and application to home-based upper limb rehabilitation," *IEEE Trans. Biomed. Eng.*, vol. 60, no. 8, pp. 2184–2192, Aug. 2013.

[14] W. Morey, G. Meltz, and H. Glenn, "Fiber optic Bragg grating sensors," in *Fiber Optic and Laser Sensors VII*, 1989, vol. 1169, pp. 98–107.